Available online at www.sciencedirect.com

ScienceDirect

Nuclear Physics A 1032 (2023) 122611

NUCLEAR PHYSICS A

www.elsevier.com/locate/nuclphysa

^{105}Rh yield from the proton induced fission of uranium

T. Najumunnisa [a,b], M.M. Musthafa [a,*], C.V. Midhun [a], Muhammed Aslam [c], K.K. Rajesh [a], P. Surendran [d], J.P. Nair [d], A. Shanbhag [e], S. Ghugre [f]

[a] *Department of Physics, University of Calicut, Malappuram, 673635, Kerala, India*
[b] *AKNM Government Polytechnic College, Tirurangadi, 676317, Kerala, India*
[c] *Government Arts and Science College, Kozhikode, 673018, Kerala, India*
[d] *BARC-TIFR Pelletron Group, BARC, Mumbai, 400085, Maharashtra, India*
[e] *Health Physics Division, BARC, Mumbai, 400085, Maharashtra, India*
[f] *UGC-DAE Consortium for Scientific Research, Kolkata, 700098, India*

Received 3 November 2022; received in revised form 28 December 2022; accepted 24 January 2023
Available online 30 January 2023

Abstract

The yield of ^{105}Ru and ^{105}Rh produced through proton induced fission of ^{238}U are measured using stacked foil activation technique. The results are compared with theoretical calculations using TALYS 1.95. As the ^{105}Rh shows a higher cross-section for neutron absorption in the thermal region, production of this isotope will act as a reactor poison. Hence the reactivity equivalent of ^{105}Rh is also calculated and is found to be -0.84%.

Keywords: Proton induced fission; Stacked foil activation analysis; Excitation function; Isotopic yield; Reactor poisoning

1. Introduction

The requirement of Nuclear data as a function of energy has significant importance in design and operation of nuclear reactors [1,2]. To account the variation of k_{eff}, the neutron produc-

* Corresponding author.
E-mail address: mmm@uoc.ac.in (M.M. Musthafa).

https://doi.org/10.1016/j.nuclphysa.2023.122611
0375-9474/

ing and absorbing reactions have to be accounted and benchmarked. A strong secondary proton spectrum is formed in the Gen IV reactors, ADS and fast neutron reactors as a result of neutron interaction on moderators, fuel, fission fragments as well as the structural components [3–5]. Energy of these proton spectrum ranges upto 20 MeV [4–6]. This is important, particularly, as the reactor functions continuously for an average period of two years with high flux. These secondary protons can induce fission on ^{238}U, resulting a mass distribution different from that of designed neutron induced fission [7]. These newly formed fragments will also interact with the neutron flux in the reactor and will affect the reactor criticality [8]. The fission product ^{105}Rh has large neutron capture cross-section similar to ^{135}Xe and is found to be having poisoning effect similar to xenon poisoning effect [9]. Hence it is necessary to analyse the fission product formed in proton induced fission of ^{238}U over energy interval of 0 – 20 MeV and their decay.

Further, most of the fission fragments so produced are radioactive materials having utilisation in the field medicine [10], industry [11] and research. In medical fields radioactive nuclides are widely used for therapy and imaging. These nuclei are generally taken from the fission fragments or produced by bombardment of neutrons, mostly from fission reactors or produced through accelerated charged particles. There is a wide range of radionuclides which are used for the therapeutic applications [12]. ^{105}Rh is one of such radioactive isotopes which is used for targeted therapy. Rh forms inert and stable complexes with a number of multidentate ligands which could be used as carrier molecules, either directly or after linking with an antibody or peptide in order to direct ^{105}Rh to the target tumour cells [13]. ^{105}Rh has a half life of 35.34 h and decays by the emission of β^- particles of 560 keV (70%) 250 keV (30%) and γ rays of 319 keV (19%) and 306 keV (5%) [14]. These features make ^{105}Rh attractive for dosimetry and pharmacokinetic applications.

In the reactor environment, ^{105}Rh is generally formed by the decay of ^{105}Ru which is the progeny of fission fragments ^{105}Nb, ^{105}Mo, and ^{105}Tc having very short half lives 2.95 s, 35.6 s and 7.6 minutes respectively. Since these fission fragments are having shorter half lives, they will decay immediately to ^{105}Ru, having moderate half life 4.4 hours. Hence in order to estimate the yield of ^{105}Rh, it is important to estimate the production of ^{105}Ru and its decay with time.

In this perspective we have measured the time dependant yield of ^{105}Ru and ^{105}Rh formed through the proton induced fission of ^{238}U. There is wide interest in measuring specific fragment production yields in $^{238}U(p, f)$, where many isotope yields are reported and compiled to EXFOR [15–20]. However these are seemed to be deduced from the assumption of first generation fission fragments only and the decay branching is not well explored.

2. Experimental analysis

The experiment has been carried out at TIFR, Mumbai, India using BARC – TIFR pelletron linac facility. Stacked foil activation technique has been employed for the experiment. Natural Uranium samples of thickness 8.6 mg/cm^2 were prepared by rolling. The stack containing three Uranium foils with energy degraders were exposed to the proton beam of 22 MeV energy. The actual stack contains various materials such as cadmium (5 mg/cm^2), aluminium (2.97 mg/cm^2 & 108.6 mg/cm^2), indium (13 mg/cm^2), copper (mg/cm^2) and uranium (8.6 mg/cm^2) as shown in Fig. 1. Since the present work is focusing on uranium only, other foils have been treated as energy degraders. The beam current was monitored continuously using current integrator connected to the secondary electrons suppressed target stack. An average proton current of 23 nA were fired on the stack for 88 minutes.

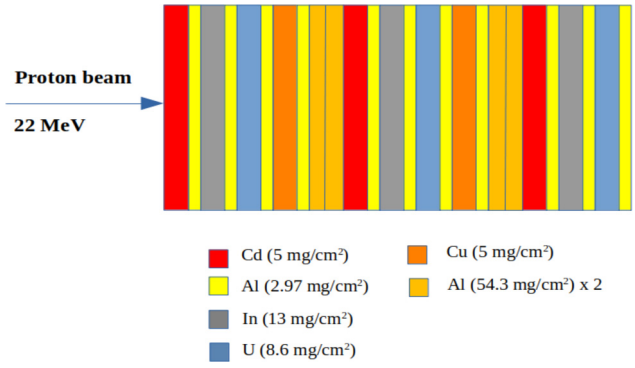

Fig. 1. Stack of Uranium samples along with energy degraders.

Mean incident energy on each sample and the energy uncertainties were calculated using the stopping power calculating code SRIM [21]. The mean incident energies are calculated as follows: First the dE/dx is calculated for the incident energy on the first foil corresponding to its thickness. The mean energy is taken as the mean value of the entrance and exit energy for this foil. This practice is followed for each foil in this stack and aluminium degraders. In the case of thick degraders, total thickness is sliced into 2-4 fragments and the energy loss is calculated for each fragment. This procedure will minimise the uncertainty in fixing the mean energy on each sample. The uncertainty in the values of mean incident energies is the rms value of the energy uncertainty due to thickness of the sample and the uncertainty due to longitudinal and lateral straggling. Mean incident energies on the three uranium samples thus calculated were 21.44 MeV, 17.24 MeV and 12.12 MeV respectively with errors as shown in Table 2. The irradiated samples were kept for some times for cooling due to strong activity induced in the sample. The first sample, corresponding to incident energy 21.44 MeV, was taken for counting after 3 hours and 43 minutes from the stoppage of irradiation.

The γ spectroscopy was performed with low background counting facility based on 100 cc HPGe detector. The HPGe detector was calibrated using standard ^{152}Eu reference source and the energy dependent efficiencies are reproduced using a quadratic function. Background spectrum was taken for 50,000 seconds before the counting of the samples. The background spectrum is shown in the Fig. 2. There is no mixing of gamma energies of interest and the background counting rate is negligibly small. Fig. 3 shows the interested portion of the gamma ray spectrum in which the following characteristic gamma rays of ^{105}Ru, viz., 724.3 keV (47.3%), 469.37 keV (17.5%) and 676.36 keV (15.7%) were identified. Similarly the gamma rays from second and third samples of Uranium were counted after 3 hours 58 minutes and 4 hours 9 minutes respectively from the stoppage of irradiation. The above mentioned gamma rays of ^{105}Ru are present in the spectra of the other two Uranium samples corresponding to the incident proton energies 17.24 MeV and 12.12 MeV also. Since the half life of ^{105}Ru is 4.44 h and is 100% β^- emitter, the ^{105}Ru will decay almost completely after typically six half life to ^{105}Rh. Inorder to get high population of ^{105}Rh, we had waited for one day and the counting was repeated again after a cooling time of 29 hours and 54 minutes. The second counting of each samples were carried out separately and the characteristic gamma rays of ^{105}Rh, viz., 318.9 keV (19.1%) and 306.1 keV (5.1%) were identified clearly. Fig. 4., shows the interested portion of the gamma ray spectrum of the Uranium sample corresponding to incident energy 21.44 MeV obtained during the second counting.

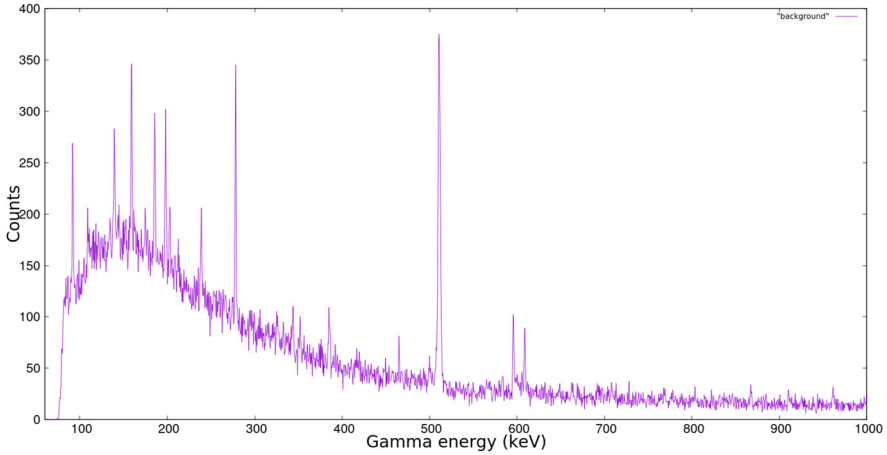

Fig. 2. Background spectrum.

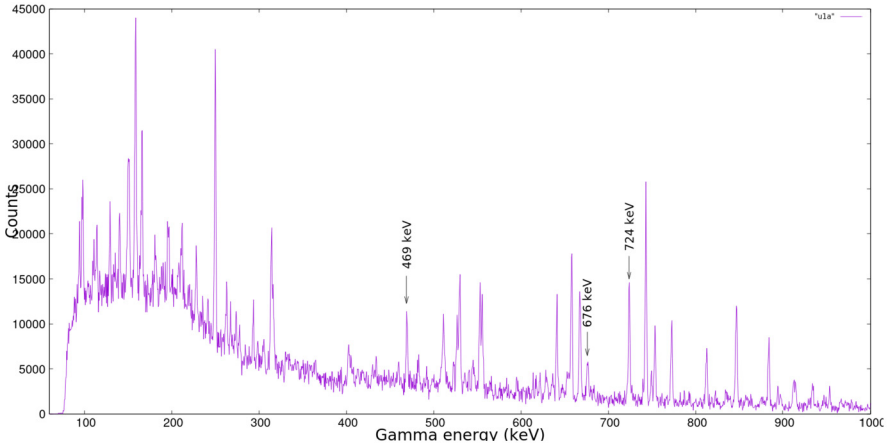

Fig. 3. Gamma ray spectrum corresponding to first counting (proton energy 21.44 MeV).

The gamma rays of ^{105}Rh were very feeble in the first counted spectrum and were well defined in the second counting. This shows that the ^{105}Rh were not formed directly during irradiation but was formed by the decay of ^{105}Ru. From the spectrum obtained during second counting, it can be seen that the characteristic gamma peaks of ^{105}Ru were almost washed out.

The fission product yields of ^{105}Ru and ^{105}Rh are measured for the incident proton energies 12.12 MeV, 17.24 MeV and 21.44 MeV. The calculations of the yields are done by the assumptions that the nuclei ^{105}Nb, ^{105}Mo and ^{105}Tc were formed as fission fragments and the half lives of these nuclei are very short and all are β^- emitters as shown in the decay scheme in Fig. 5. These all nuclei undergo β^- decay and ^{105}Ru and ^{105}Rh were formed through these decay chain. Since the half lives of the above mentioned nuclei are extremely short (few seconds and minutes) (Table 1) when compared to the irradiation time, practically it is assumed that the ^{105}Ru is formed during the irradiation itself and based on this assumption, we have calculated the cross-section of the formation of ^{105}Ru from the observed gamma ray spectrum of the irradiated

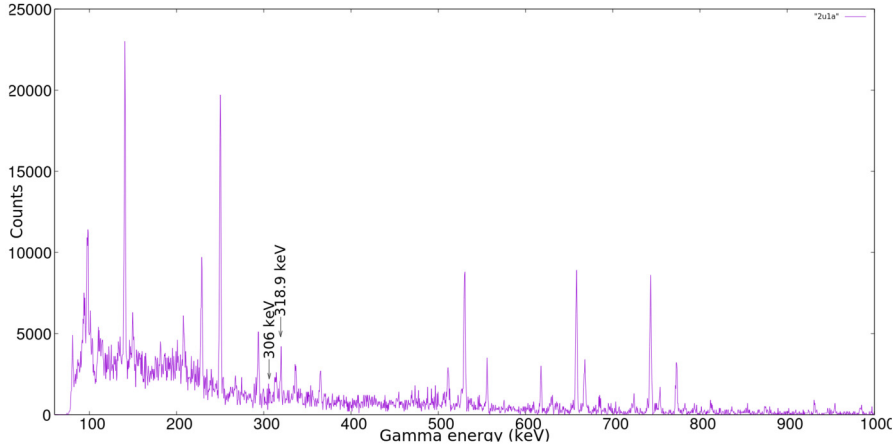

Fig. 4. Gamma ray spectrum corresponding to second counting (proton energy 21.44 MeV).

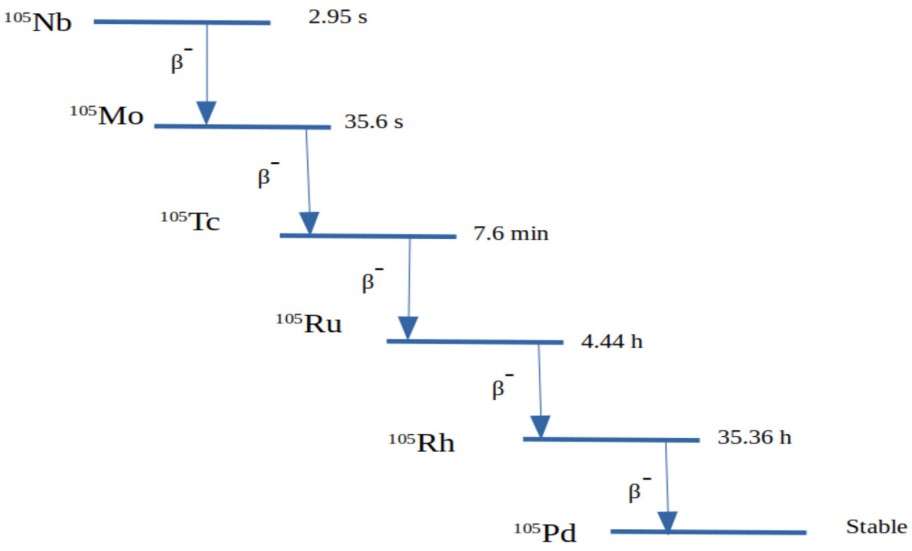

Fig. 5. Decay chain of ^{105}Nb.

Table 1
Half lives of the interested fission fragments.

Fission Fragments	$t_{1/2}$
^{105}Nb	2.95 s
^{105}Mo	35.6 s
^{105}Tc	7.6 min
^{105}Ru	4.44 h
^{105}Rh	35.36 h

Table 2
Measured yields of ^{105}Ru and ^{105}Rh.

Residual nucleus	Incident proton energy (MeV)	Yield (mb)
^{105}Ru	12.12 ± 0.57	1.41 ± 0.29
	17.24 ± 0.75	3.38 ± 0.29
	21.44 ± 0.91	5.09 ±0.27
^{105}Rh	12.12 ± 0.57	0.52 ± 0.19
	17.24 ± 0.75	2.18 ± 0.56
	21.44 ± 0.91	2.17 ± 0.36

sample where as in the theoretical calculation, it is considered that ^{105}Ru is formed as the decay product of decay chain starting from ^{105}Nb. The yield of ^{105}Rh is calculated by accounting the decay probability of ^{105}Ru The production cross-section for the formation of isotope of interest from the observed count of the characteristic gamma ray is calculated using the equation (1) [22].

$$\sigma = \frac{A\lambda exp(\lambda t_2)}{\phi.N_o\,[1 - exp(-\lambda t_1)]\,[1 - exp(-\lambda t_3)]\,G\varepsilon.\theta.k} \tag{1}$$

Where A represents the total number of activities counted under the corresponding gamma peak, λ is the decay constant of the particular residual nucleus, ϕ is the incident proton flux, N_0 is the number of the target nuclear isotope per unit area of the irradiated sample, G_ε is the geometry dependent efficiency of the detector for the given gamma ray energy, θ is branching ratio of the particular gamma ray, k is the self-absorption correction factor for the gamma ray in the sample and t_1, t_2, t_3 are respectively the irradiation time, the cooling time and the counting time of the sample. The decay constant λ is taken from the IAEA-NDS website [14].

^{105}Rh being produced as the decay product of ^{105}Ru, the activity of ^{105}Rh is calculated using the equation (2) [23] given below

$$A_d(t) = A_p(t)\frac{\lambda_d}{\lambda_d - \lambda_p}(1 - exp(-(\lambda_d - \lambda_p)t)) \tag{2}$$

where $A_d(t)$ is the activity of the daughter nucleus and $A_p(t)$ is the activity of the parent nucleus at time t and λ_d and λ_p are the decay constants of daughter and the parent nuclei respectively. The yields of ^{105}Ru and ^{105}Rh thus calculated are shown in Table 2.

In the present measurement, the following factors may be responsible for errors: 1) The statistical error of gamma counting. 2) Errors arising from the estimation of number of target nuclei due to inaccurate estimate of foil thickness and nonuniform deposits of target material. 3) The beam current may fluctuate during the irradiation which results in the variation of incident flux. Since the irradiation time is shorter and the half life of the fragments are in hours only, we have neglected this error. 4) The measured detection efficiency of the detector may be inaccurate on accounting the statistical errors of gamma ray counting of a standard source. This was minimised by taking counts for larger time ($\approx$ 3600 sec). Detailed error analysis of such measurement is given elsewhere [24,25].

3. Analysis of the data

Theoretical analysis of the data for the production of ^{105}Ru and ^{105}Rh from $^{238}U(p, f)$ has been performed with the nuclear reaction model code, TALYS 1.95 [26]. In TALYS, the default model implemented for fission is based on the transition state hypothesis of Bohr [27]

and the Hill-Wheeler [28] expression. This gives transmission coefficients that enter the Hauser-Feshbach model to compete with the particle and photon transmission coefficients. Fission barrier parameters are calculated using experimental parameters [29]. Fission fragment calculation has been done using GEF model [30] and Temperature-dependent Brosa model [31]. The fission fragment mass distribution is determined with a revised version of the multi-modal random neck-rupture model (MM-RNRM) [32]. MM-RNRM gives information on the mass yields of the fission fragments only. Predictions of charge distributions are performed in TALYS within the scission-point-model-like approach [33].

The default optical model potential parameterisations of Koning and Delaroche [34] has been employed here. For the compound nuclear model calculations, Hauser-Feshbach model [35] with width fluctuation correction (WFC) [36] formalism is used. In the present calculation, the pre-equilibrium part has been done using exciton model [37] in which the default two-component model is considered in the calculation. The fission barrier is calculated using the experimental fission barrier parameters which are the collection of a large set of actinide fission barrier heights and curvatures for both the inner and outer barrier based on a fit to experimental data. Constant temperature model [38] and Fermi gas model are used for level density calculations.

The measured yield of the fission fragments ^{105}Ru and ^{105}Rh during the proton induced fission of uranium are compared with TALYS calculations. TALYS calculations give only the production cross-section for the formation of ^{105}Nb, ^{105}Mo and ^{105}Tc and the isotopes ^{105}Ru and ^{105}Rh are not formed directly. The measured values are comparable with the values calculated by considering that the nuclei ^{105}Ru and ^{105}Rh are formed through the decay channel given in the Fig. 4. This shows that the produced nuclei ^{105}Ru and ^{105}Rh are coming after successive beta decays of ^{105}Nb, ^{105}Mo and ^{105}Tc and not through direct formation. The time dependent yield of ^{105}Ru and ^{105}Rh are thus calculated from the cross-section data of the above mentioned isotopes, as detailed below.

The yield of ^{105}Ru is calculated by considering that ^{105}Nb, ^{105}Mo and ^{105}Tc are produced as fission fragments and they will decay individually to ^{105}Ru. That is, the fission fragment ^{105}Nb ($t_{1/2}$ = 2.95 s) (Table 1) undergoes beta decay to ^{105}Mo and this ^{105}Mo ($t_{1/2}$ = 35.6 s) decay to ^{105}Tc ($t_{1/2}$ = 7.6 min) and finally the ^{105}Tc decay to ^{105}Ru ($t_{1/2}$ = 4.44 h). Also the decay series from the fission fragments ^{105}Mo to ^{105}Ru and from ^{105}Tc to ^{105}Ru are considered separately and the yields obtained from all these three decay series are added to get the yield of ^{105}Ru. This is important as the irradiation time and cooling time are much longer than the half lives of ^{105}Nb, ^{105}Mo and ^{105}Tc. The yield of ^{105}Rh is calculated from the beta decay of ^{105}Ru. Thus obtained yields are comparable to the measured yield of these isotopes for each energy point. In this decay chain, the half-lives of daughter nuclei is greater than the half-lives of the parent nuclei (non-equilibrium condition). During the calculation the yield of daughter nucleus (^{105}Rh) is calculated using the equation (2). Since the half-lives of the isotopes ^{105}Nb, ^{105}Mo and ^{105}Tc are few seconds, the time t used in the calculation of yield upto ^{105}Tc in the above equation is the time for the maximum activity obtained using the equation

$$t_{max} = \frac{1}{\lambda_d - \lambda_p} ln(\frac{\lambda_d}{\lambda_p}) \tag{3}$$

4. Result and discussions

The fission fragment yields of ^{105}Ru and ^{105}Rh formed through proton induced fission of natural Uranium are measured for the proton energies 21.12 MeV, 17.24 MeV and 21.44 MeV.

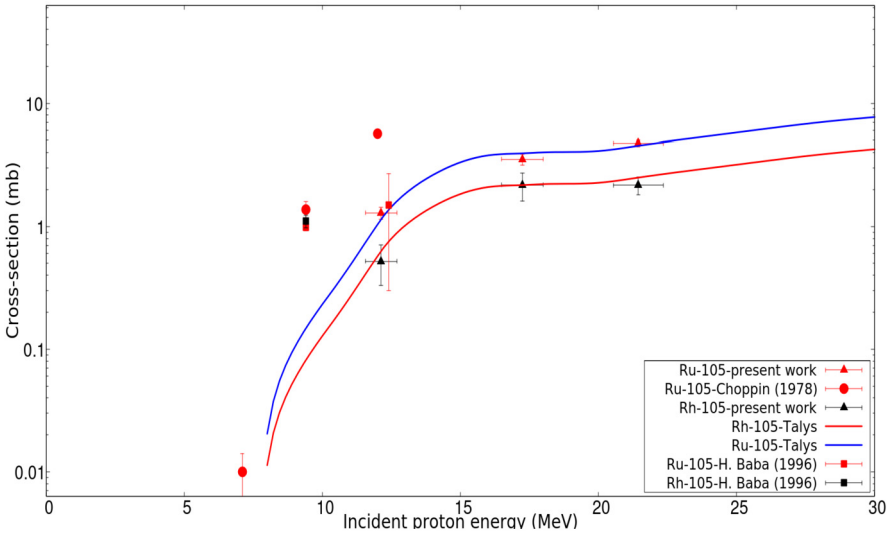

Fig. 6. Excitation function for the formation of ^{105}Ru and ^{105}Rh.

The results are given in Table 2. The excitation function for the formation of ^{105}Ru and ^{105}Rh are plotted along with the TALYS calculation and are shown in the Fig. 6. The reported data [17,22] available in EXFOR library are also given. It is clear that the measured data exactly matching with the calculated data. From this it can be confirmed that the produced nuclei ^{105}Ru and ^{105}Rh are formed through the successive beta decay of ^{105}Nb, ^{105}Mo and ^{105}Tc and not by direct production. From the figure, it can be seen that the cross-section data of ^{105}Ru reported by H. Baba et al. [22] corresponding to proton energy 12.4 MeV exactly matches the present measurement. But the data corresponding to proton energy 9.4 MeV stay far from the TALYS calculation. The data reported by Choppin et al. [17] are found to be over-estimating the present calculations. There is no straight forward comment to be offered on these discrepancies. However it is to be noted that they have reported as the cumulative cross-sections corresponding to each energy.

The isotopes ^{105}Ru and ^{105}Rh produced due to the fission of Uranium in nuclear reactor may interact with neutrons formed during fission and may show poisoning effect similar to xenon poisoning. So we have calculated the neutron capture cross-sections of these nuclei from thermal upto 10 MeV using TALYS and are plotted in Fig. 7. The neutron capture cross-section of ^{135}Xe for the same energy range along with reported data [39] is also included in the plot for comparison. For the sake of completeness, it is also calculated the neutron capture cross-section of the precursors of ^{105}Ru and ^{105}Rh such as ^{105}Nb, ^{105}Mo and ^{105}Tc and are also shown in the Fig. 7. In TALYS calculation, default input parameters are used. As can be seen from this figure, ^{105}Rh shows significant cross-section for neutron absorption in thermal energy region. The absorption cross-section of ^{105}Rh at 20^0C (0.0253 eV) is 2.1 x10^4 b. Further, the excitation function shows similar behaviour as that of ^{135}Xe and is found that the neutron capture of ^{105}Rh is comparable to that of ^{135}Xe beyond neutron energy 1 eV.

The reactivity of a reactor describes the deviation of an effective multiplication factor from unity. For critical conditions, the reactivity should be zero. The larger the absolute reactivity

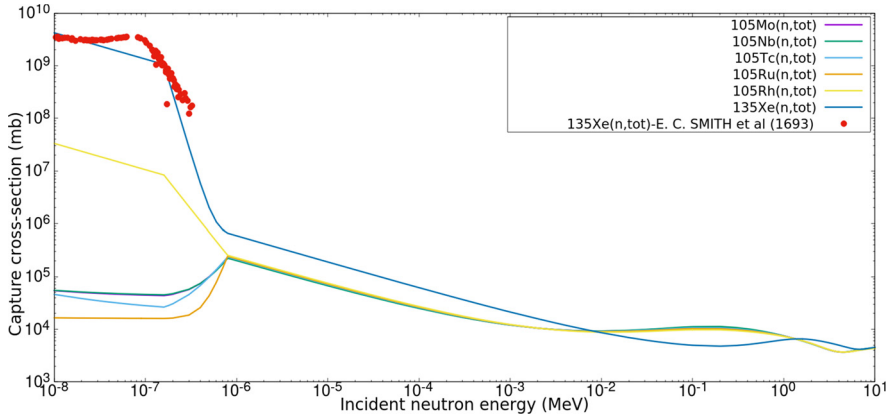

Fig. 7. Neutron capture cross-section of ^{105}Nb, ^{105}Mo, ^{105}Tc, ^{105}Ru and ^{105}Rh along with ^{135}Xe.

value in the reactor core, the farther the reactor is from criticality. The reactivity ρ equivalent of any poison in a reactor can be calculated by the equation (4) [11] given below

$$\rho = -\frac{\bar{\Sigma}_{aP}/\bar{\Sigma}_f}{\nu p \epsilon} \tag{4}$$

where $\bar{\Sigma}_{aP}$ is the macroscopic neutron absorption cross-section of the poison, $\bar{\Sigma}_f$ is the macroscopic fission cross-section, ν is the average number of neutrons produced per fission, p is the resonance escape probability and ϵ is the fast fission factor. While calculating the reactivity equivalent of ^{105}Rh it is assumed that the reactor is fuelled with ^{235}U only and contains no resonance absorbers. In nuclear reactor fuelled with ^{235}U, typical enrichment will be 3-5%. Hence the major content will be still ^{238}U (95%). In this case $p = \epsilon = 1$. The reactivity obtained for ^{105}Rh is -0.84%. If the reactor contains resonance absorbers, the reactivity will be somewhat higher.

5. Conclusion

The fission fragment yields of ^{105}Ru and ^{105}Rh produced through proton induced fission of ^{238}U are experimentally measured. The experimentally obtained yields are compared with literature data and theoretical calculation by TALYS 1.95. The TALYS calculations reproduce the measured data assuming that ^{105}Ru, ^{105}Rh are not produced directly as fission fragments. The observations indicate that the these ^{105}Ru and ^{105}Rh are formed through the beta decay of fission fragments ^{105}Nb, ^{105}Mo and ^{105}Tc. The reactivity equivalent of ^{105}Rh is found to be -0.84%.

CRediT authorship contribution statement

T. Najumunnisa: Conceptualization, Formal analysis, Investigation, Methodology, Visualization, Writing – original draft. **M.M. Musthafa:** Supervision, Writing – review & editing. **C.V. Midhun:** Software. **Muhammed Aslam:** Resources. **K.K. Rajesh:** Resources. **P. Surendran:** Resources. **J.P. Nair:** Resources. **A. Shanbhag:** Resources. **S. Ghugre:** Resources.

Declaration of competing interest

The authors declare that they have no known competing financial interests or personal relationships that could have appeared to influence the work reported in this paper.

Data availability

Data will be made available on request.

Acknowledgements

The work is a part of UGC-DAE CSR project No. UGC-DAE-CSR-KC/CRS/13/NP03, sanctioned to MMM. The authors acknowledge A. Saxena, Nuclear Physics Division, BARC for providing Uranium target. The authors acknowledge the support of E Krishnakumar, Vandana Nanal and other scientific and technical team of the TIFR, Mumbai during the conduct of experiment.

References

[1] S. Ganesan, Invited talk, in: International Conference on Nuclear Data ND2004, Santa Fe, USA, in: American Institute of Physics (AIP) Conference Proceedings CP769, May 2005, pp. 1411–1416.
[2] S. Ganesan, Invited talk, in: Nuclear Physics & Astrophysics at CERN (NuPAC), CERN, Geneva, Switzerland, Oct. 10–12, 2005.
[3] Masato Takahashi, Shungo Iijima, J. Nucl. Sci. Technol. 26 (9) (September 1989) 874–880.
[4] Jyoti Pandey, et al., Phys. Rev. C 99 (2019) 014611.
[5] Ramandeep Gandhi, et al., Phys. Rev. C 100 (2019) 054613.
[6] P.D. Hondt, C. Wagemans, A. Declercq, G. Barreau, A. Deruytter, Nucl. Phys. A 346 (1980) 461–472.
[7] Swapna Balakrishnan, M.M. Musthafa, C.V. Midhun, in: Proceedings of the DAE Symp. on Nucl. Phys., 2022.
[8] S. Ganeshan, Pramana J. Phys. 68 (2) (February 2007) 257–268.
[9] John R. Lamarsh, Anthony J. Baratta, Introduction to Nuclear Engineering, Third Edition, 1982, p. 934.
[10] Fission molybdenum for medical use, Proceedings of a technical committee meeting organized by the international atomic energy agency and held in Karlsruhe, 13-16 October 1987.
[11] N. Ramamoorthy, M. Haji-Saeid, in: Proceedings of the Third Eurasian Conference "Nuclear Science and Its Application", October 5-8, 2004.
[12] M. Neves, A. Kling, A. Oliveira, J. Radioanal. Nucl. Chem. 266 (3) (2005) 377–384.
[13] P.R. Unni, K. Kothari, M.R.A. Pillai, in: Proceedings of an International Seminar held in Hyderabad, India, 18-22 January 1999, p. 90.
[14] Live chart, IAEA-NDS, https://www-nds.iaea.org/relnsd/vcharthtml/VChartHTML.html.
[15] G.R. Choppin, E.F. Meyer jr., J. Inorg. Nucl. Chem. 28 (1966) 1509–1518.
[16] G.R. Choppin, A.T. Kandil, J. Inorg. Nucl. Chem. 34 (1972) 439–442.
[17] R.W. Eaker, A.T. Kandil, G.R. Choppin, J. Inorg. Nucl. Chem. 38 (1976) 969–973.
[18] H. Kudo, M. Maruyama, M. Tanikawa, T. Shinozuka, M. Fujioka, Phys. Rev. C 57 (1) (January 1998).
[19] E. Karttunen, M. Brenner, V.A. Rubchena, S.A. Egorov, V.B. Funschtein, V.A. Jakovlev, Yu.A. Selitskiy, Nucl. Sci. Eng. 109 (1991) 350–359.
[20] H. Baba, et al., Z. Phys. Hadrons Nucl. 356 (1) (1996) 61–70.
[21] J.F. Ziegler, Pergamon Press, 1977–1985, pp. 2–6.
[22] M.M. Musthafa, Manoj Kumar Sharma, B.P. Singh, R. Prasad, Appl. Radiat. Isot. 62 (3) (2005) 419–428.
[23] Craig Levin, Emis. Tomogr. 816 (2004) 53–88.
[24] B.P. Singh, M.G.V. Sankaracharyulu, M. Afzal Ansari, H.D. Bhardwaj, R. Prasad, Phys. Rev. C 47 (1993) 2055.
[25] M.M. Musthafa, B.P. Singh, M.G.V. Sankaracharyulu, H.D. Bhardwaj, R. Prasad, Phys. Rev. C 52 (1995) 6.
[26] A.J. Koning, S. Hilaire, M.C. Duijvestijn, in: O. Bersillon, F. Gunsing, E. Bauge, R. Jacqmin, S. Leray (Eds.), Proceedings of the International Conference on Nuclear Data for Science and Technology, April 22-27, 2007, Nice, France, EDP Sciences, 2008, pp. 211–214.

[27] N. Bohr, Phys. Rev. 56 (1939) 426.
[28] D.L. Hill, J.A. Wheeler, Phys. Rev. 89 (1953) 1102;
T.D. Thomas, Phys. Rev. 116 (1959) 703.
[29] R. Capote, et al., RIPL – reference input parameter library for calculation of nuclear reactions and nuclear data evaluation, Nucl. Data Sheets 110 (2009) 3107.
[30] K.H. Schmidt, B. Jurado, C. Amouroux, C. Schmitt, Nucl. Data Sheets 131 (2016) 107–221.
[31] U. Brosa, S. Großmann, A. Müller, Phys. Rep. 197 (1990) 167.
[32] M.C. Duijvestijn, A.J. Koning, F.-J. Hambsch, Phys. Rev. C 64 (2001) 014607.
[33] B.D. Wilkins, E.P. Steinberg, R.R. Chasman, Phys. Rev. C 14 (1976) 1832.
[34] A.J. Koning, J.P. Delaroche, Nucl. Phys. A 713 (2003) 231.
[35] W. Hauser, H. Feshbach, Phys. Rev. 87 (1952) 366.
[36] P.A. Moldauer, Phys. Rev. C 14 (1976) 764.
[37] A.J. Koning, M.C. Duijvestijn, Nucl. Phys. A 744 (2004) 15.
[38] A. Gilbert, A.G.W. Cameron, Can. J. Phys. 43 (1965) 1446.
[39] E.C. Smith, G.S. Pawlicki, P.E.F. Thurlow, G.W. Parker, W.J. Martin, G.E. Creek, P.M. Lantz, S. Bernstein, Phys. Rev. 115 (1693).